Oscillatory interlayer coupling in Fe/Mn/Fe trilayers

Shi-shen Yan
Institut für Festkörperforschung, Forschungszentrum Jülich GmbH, D-52425 Jülich, Germany
and Department of Physics, Shandong University, Jinan, Shandong 250100, People's Republic of China

R. Schreiber, F. Voges, C. Osthöver, and P. Grünberg
Institut für Festkörperforschung, Forschungszentrum Jülich GmbH, D-52425 Jülich, Germany
(Received 13 November 1998)

Fe/Mn/Fe wedged-shape sandwiches were prepared by molecular beam epitaxy under optimal conditions. The interlayer coupling measured by magneto-optic Kerr effect is very strong for thin Mn layers. The canted angle between the magnetization vectors of the two magnetic layers in remanence increases gradually from 0° to about 180° and then gradually reduces to 90° for Mn thicknesses from 0.62 to 1.2 nm. For Mn layer thicknesses in the range between 1.2 and 2.45 nm, the interlayer coupling is always 90° coupling, but its strength oscillates with a short period of about 2 Mn monolayers. The above coupling phenomenon can be well described by the proximity magnetism model. [S0163-1829(99)50618-8]

Recently the mechanisms which couple ferromagnetic (FM) films across antiferromagnetic (AF) metallic interlayers have been of great interest. For AF interlayers one would expect a large contribution to the coupling coming from the direct nearest-neighbor exchange inside the interlayers and across the interfaces but since they are metals the indirect interaction due to the conduction electrons could be considered in addition. We consider here AF interlayers polarized in the plane of the film with sheets alternatively parallel and antiparallel to the magnetization of the FM films as observed by Walker and Hopster[1] on overlayers of Mn grown on Fe. In the ideal case one would expect oscillations of the coupling strength with a period of two monolayers (ML), with large amplitudes and sign changes.

While this behavior has been studied in much detail for Cr interlayers and even a magnetic phase diagram for the Cr interlayer was deduced[2] which explains most of the experimental results, for Mn interlayer the situation is less clear. In the first work on Fe/Mn/Fe trilayers[3] Purcell *et al.* found interlayer coupling oscillations with a two ML period but there were no sign changes, indicating an appreciable background of AF coupling. On the contrary, Filipkowski *et al.*[4] found very strong near-90° coupling with no evidence for AF coupling in their CoFe/Mn/CoFe samples at room temperature. Also in contrast to the results in Fe/Mn/Fe trilayers,[3] the two ML period oscillations were absent in Co/Mn (Ref. 5) and Fe/Mn (Ref. 6) multilayers. Furthermore, the interlayer coupling in epitaxial Co/Mn multilayers[7] was attributed to the AF order of the Mn spacer. Unfortunately, the authors did not show the dependence of the interlayer coupling on the Mn layer thickness.

In view of these contradictory results the aim of the present work was to prepare samples of the best possible quality which could provide reliable information on the coupling in this interesting system. Since this work and the evaluation of the experiments will be based on the assumption that we are here dealing with AF Mn as interlayer material we will use Slonczewki's proximity magnetism model[8] for the evaluation of the experiments. It will be briefly introduced in the next paragraph and compared with the usual method to evaluate such experiments.

The proximity magnetism model[8] is a phenomenological model for the description of exchange coupling across AF materials including thickness fluctuations due to interface roughness. According to Slonczewski[8] the exchange coupling energy per unit area can be written as

$$E_c = C_+(\theta)^2 + C_-(\theta-\pi)^2, \tag{1}$$

where $C_+ \geqslant 0$, $C_- \geqslant 0$ and $0 \leqslant \theta \leqslant \pi$. Here C_+ and C_- are the coupling coefficients, and θ is the angle between the magnetization vectors of the two FM layers (here Fe). This contrasts with another phenomenological energy expression which was previously used exclusively in work on interlayer coupling:

$$E_c = -j_1\cos(\theta) - j_2\cos^2(\theta). \tag{2}$$

Here θ as above is the angle between the magnetization vectors of the FM layers. The first term with the parameter j_1 represents the bilinear coupling and the second term with j_2 describes the 90° coupling. It is now believed that Eq. (1) is appropriate for interlayers with static magnetic order and Eq. (2) for those which consist of a diamagnetic or paramagnetic material. Experimentally the difference between Eq. (1) and Eq. (2) shows up in a subtle difference concerning saturation after remagnetization. Where Eq. (2) implies full saturation is reached at a finite critical external field, Eq. (1) implies asymptotic approach toward saturation.

The Fe/Mn/Fe wedged-shape sandwiches were deposited in UHV by thermal evaporation onto a GaAs/Fe (1 nm)/Ag (150 nm) substrate-buffer system as described elsewhere.[9–11] First a 5-nm Fe layer was grown at room temperature for the first 4 ML and at 200 °C for the rest. The Mn film was prepared with a growth rate of about 0.9 nm per minute at different temperatures between −150 °C and 200 °C, in order to find the optimal growth temperature. Taking into account both the observation of the interlayer coupling and the characterization of the structure, we found the optimal growth

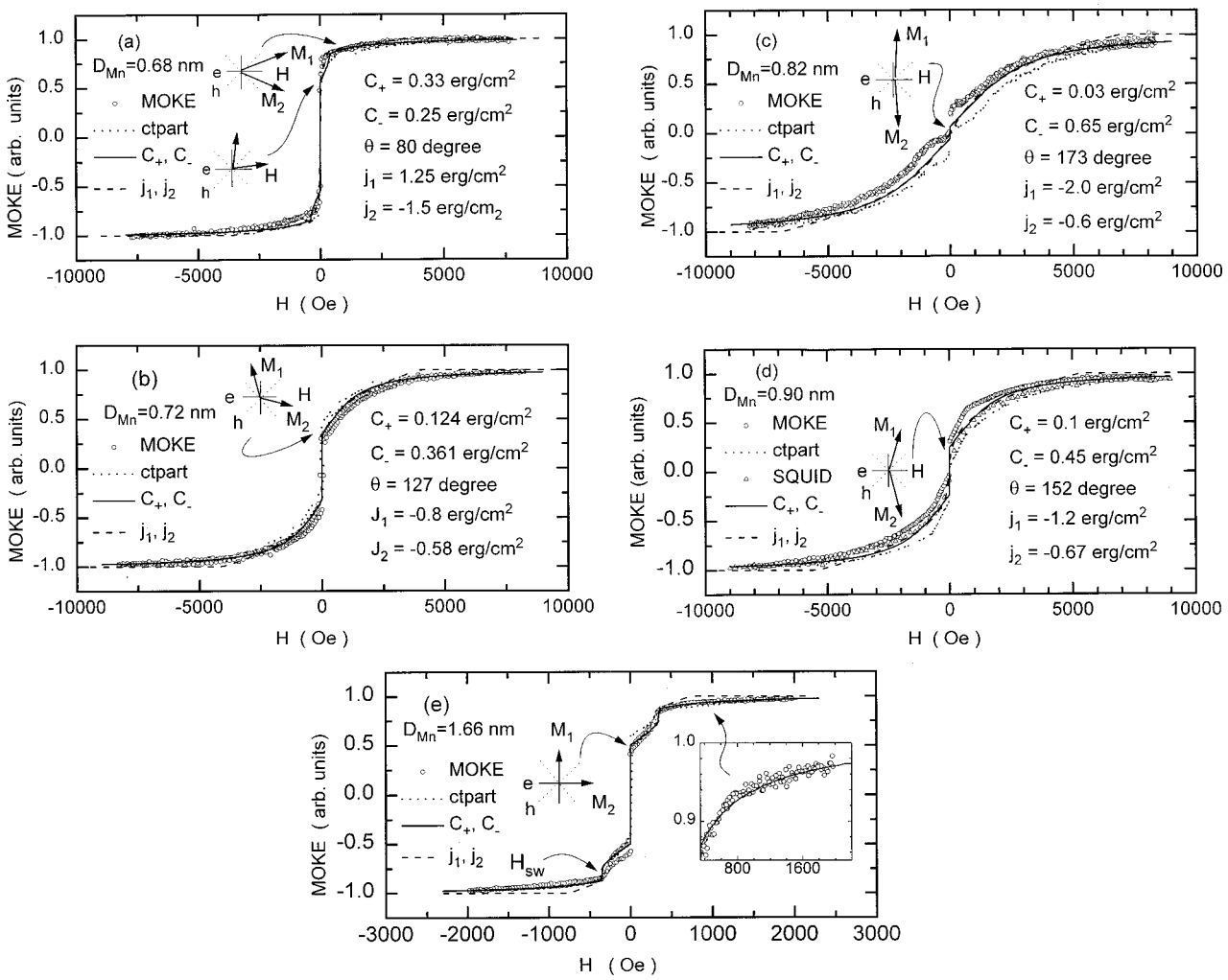

FIG. 1. Some typical hysteresis loops at room temperature and their evaluation. Open circles are experimental points obtained by MOKE and the same for triangles by SQUID. ctparts indicates the counterparts as described in the text. C_+, C_- gives fits based on Eq. (3) and the same for j_1, j_2 based on Eq. (2). D_{Mn} (nm) denotes the thickness of the Mn layer, C_+ and C_- (erg/cm^2) are the coupling coefficients, θ (degree) is the coupling angle, and j_1 and j_2 (erg/cm^2) are the parameters of Eq. (2). For (e), we use $D_{\mathrm{Mn}}=1.66$ nm, $C_+=0.118$ erg/cm^2, $C_-=0.118$ erg/cm^2, $\theta=90°$, $j_1=0$, and $j_2=-0.28$ erg/cm^2. The inset in (e) shows the details of the hysteresis loop in the high-field range measured by MOKE and the fitting based on Eq. (3). The spin configurations in remanence are also shown schematically by inset symbols.

temperature for the Mn layers to be around 50 °C. The same growth temperature for Mn layers on Fe was also adopted by Purcell *et al.*[3] The Mn thickness was varied between 0 and 4 nm. Finally, the top 5 nm Fe were prepared at 200 °C, and a protective and antireflective 50 nm ZnS layer was deposited at room temperature. For Fe/Mn/Fe trilayers grown under the above conditions, low-energy electron diffraction (LEED), reflection high-energy electron diffraction (RHEED) and Auger analyses indicated that the single crystal quality is good, the growth is epitaxial and layer by layer, the interdiffusion is very small, and the surface is clean.

In order to evaluate the interlayer coupling we measured hysteresis loops via the longitudinal magneto-optic Kerr effect (MOKE) and in a few cases by means of superconducting quantum interference device (SQUID) magnetometry. The metal films are thin enough so the Kerr-effect measurement is sensitive to both Fe layers. The external field was applied along the easy axis in the [100] direction, and parallel to both the sample plane and the plane of incidence of the laser. In Fig. 1 we show some typical hysteresis loops for increasing Mn thicknesses, which were measured by MOKE (open circles) and SQUID (triangles) at room temperature. The interlayer coupling is very strong for thin Mn layers and its maximum is expected to be around a Mn thickness of 0.82 nm (5 ML) as shown in Fig. 1(c).

In order to obtain a more quantitative information we have modeled these loops by applying the proximity magnetism model [Eq. (1)] with the following assumptions. In Fe/Mn/Fe trilayers, the Fe magnetizations are assumed to lie parallel to the film plane, and so there is no static demagnetizing field. We also assume that the spins within an individual Fe layer remain parallel to one another because of a strong intralayer-exchange coupling. In our case, the sample plane is parallel to (001) crystallographic plane and the external field along the in-plane easy axis ([100] direction or equivalent). Taking into account the cubic anisotropy energy of Fe, Zeeman energy and interlayer coupling energy in the form of Eq. (1), we write the total energy E per unit area in the following form:

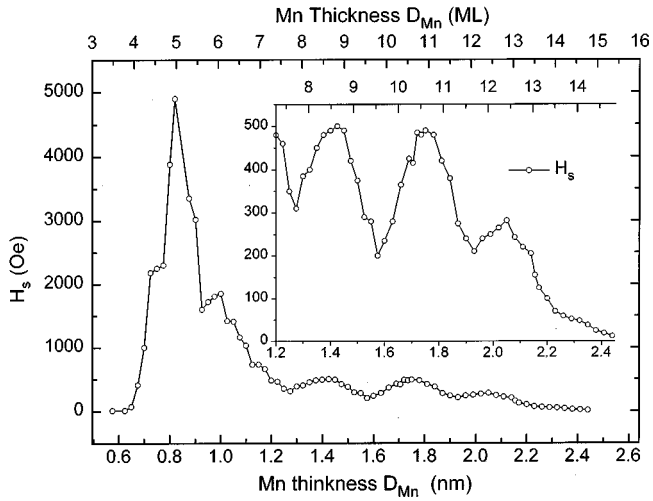

FIG. 2. The Mn layer thickness D_{Mn} dependence of the saturation field H_S. The inset shows the details of the saturation field oscillations.

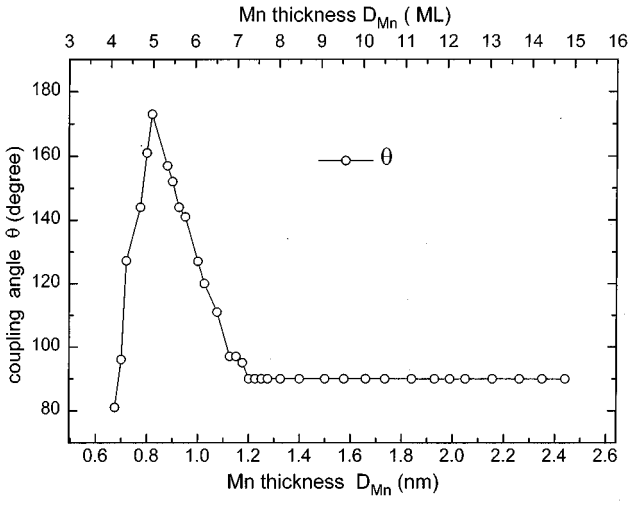

FIG. 3. The Mn layer thickness D_{Mn} dependence of coupling angle θ in remanence.

$$E = E_a + E_h + E_c,$$

$$E_a = Kt[\sin 2\Phi_1)^2 + (\sin 2\Phi_2)^2]/4,$$

$$E_h = -HMt(\cos\Phi_1 + \cos\Phi_2), \tag{3}$$

$$E_c = C_+(|\Phi_1 - \Phi_2|)^2 + C_-(|\Phi_1 - \Phi_2| - \pi)^2,$$

where E_a is the anisotropy energy, E_h is the Zeeman energy, and E_c is the interlayer coupling energy of the proximity magnetism model.[8] Here t, M, K, and H are, respectively, the thickness of the Fe layers, the saturation magnetization of the Fe layers, the first-order cubic crystal anisotropy of the Fe layers, and the external field; Φ_1 (or Φ_2) is the angle between the magnetization vector of the first (or second) Fe layer and the field direction; C_+ and C_- are the adjustable coupling coefficients, measuring the strength of the coupling. $|\Phi_1 - \Phi_2| = \theta$ $(0 \leqslant \theta \leqslant \pi)$ is the angle between the two magnetization vectors of the Fe layers at a given external field (we call it coupling angle).

The theoretical magnetization curves are obtained by minimizing the total energy of Eq. (3) with respect to Φ_1 and Φ_2 at a given external field for the appropriate C_+ and C_-. By fitting in this way the theory to the experiments, we have determined the coupling coefficients C_+ and C_-, and the coupling angle $\theta = |\Phi_1 - \Phi_2|$ at any given external field. The solid lines in the various panels of Fig. 1 show the calculated magnetization curves. For all calculations the bulk values of $M = 1707$ G and $K = 4.76 \times 10^5$ erg/cm^3 are used. The calculated magnetization curves are in good agreement with the experiments apart from the hysteresis effect and small asymmetry about the origin (0,0) introduced possibly by the second-order magneto-optic effect.[12] Since hysteresis causes in the experiments only displacements symmetrical to the zero field axis, it can easily be eliminated.

In order to get a feeling for the asymmetry in Fig. 1 the counterparts (ctpart) of the experimental MOKE hysteresis loops about the origin (0,0) are also shown by dotted lines, which are obtained by inverting the values (H,M) to $(-H, -M)$. We can see that the small asymmetry only exists in a relatively small field range. So it will be neglected in the following.

For comparison we have also used Eq. (2) by adjusting j_1 and j_2 to describe the experiments. As expected the fitting based on Eq. (2) is not very good, particularly in the high field region. As mentioned above, Eq. (2) predicts full saturation of the M-H curve at a finite external field but Eq. (1) predicts asymptotic approach towards saturation, as seen in all panels of Fig. 1. By the way, if we suppose that there exists a distribution of (j_1, j_2) in a wide region so that we can fit the experimental data well, it means that the interface roughness of the sample is large. It does not seem to be reasonable that a sample showing strong coupling and short period oscillations (will be reported in the following paragraphs) has a large roughness. In fact, Auger, LEED, and RHEED experiments indicate that the sample is of good quality. For the same reason, if the distribution of (j_1, j_2) is in a wide region, the distribution of (C_+, C_-) should also be in a wide region so that only a set of (C_+, C_-) is not enough to fit the experimental data. In fact, one set of (C_+, C_-) is enough.

Comparison with the calculations allows the interpretation of the loops with respect to the orientations of the magnetizations, as indicated for selected field values in the various panels of Fig. 1. Note in particular that in Fig. 1(e), the remanent magnetization of about half the saturation value and the large jump at near zero field indicate that the individual magnetizations switch between different easy axes but the angle between them remains 90°. For the angles between the two magnetizations in the remanent states we obtain 80°, 127°, 173°, and 152° in Figs. 1(a), 1(b), 1(c), and 1(d), respectively. Roughly the coupling gradually changes from FM to very strong near AF as shown in Fig. 1(c), and then to weak 90°-type as shown in Fig. 1(e). Further details will be reported in the following paragraph.

The strength of the interlayer coupling as represented by the saturation field H_s is shown in Fig. 2 as a function of the thickness of Mn layer, D_{Mn}. Here H_S is defined as the field at which the magnetization reaches 83% of the value ob-

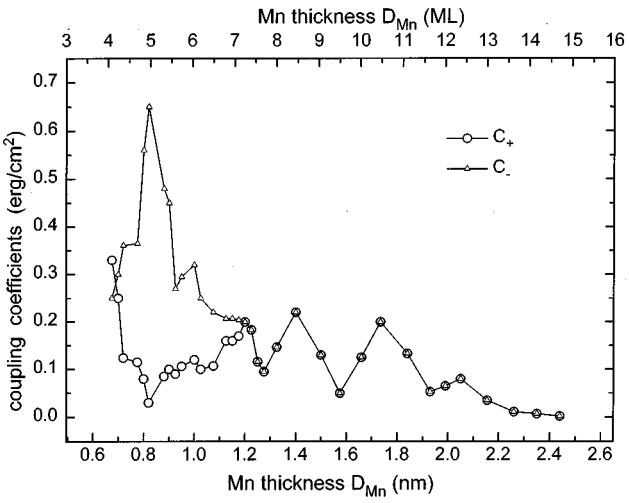

FIG. 4. The dependence of coupling coefficients C_+ and C_- on the Mn layer thickness D_{Mn}.

tained at 8000 Oe. For $D_{\mathrm{Mn}}>1.2$ nm, the coupling is weak ($H_S<500$ Oe) and H_S is very close to the switching field H_{sw} as defined in Fig. 1(e). At H_{sw} there is a large jump in the *M-H* curve, which indicates the two magnetizations become aligned symmetrical to the external field. For $D_{\mathrm{Mn}}>1.2$ nm the difference between H_S and H_{sw} is less than 10 Oe, so we use H_{sw} to replace H_S. From Fig. 2, we see that the saturation field increases drastically and then reduces quickly if the Mn thickness increases from 0.62 to 1.2 nm. If D_{Mn} further increases from 1.2 to 2.45 nm, we see obvious oscillations with a short period of about 2 Mn monolayers (about 0.33 nm). These oscillations are neither oscillations in strength of AF coupling as shown in Ref. 3 nor oscillations from FM to AF coupling. They are oscillations in the strength of 90° coupling as indicated by the shapes of the hysteresis loops, such as displayed in Fig. 1(e). So far similar oscillations were only reported by Purcell *et al.*[3] but they did not recognize the aspect that we are dealing here with 90°-type coupling.

Figure 3 shows the Mn thickness dependence of the coupling angle θ in the remanent state. The fitting procedure to obtain θ has been described above. The result shows that θ increases gradually from 0° to about 180° and then gradually reduces to 90°. For D_{Mn} between 1.2 and 2.45 nm θ is always 90°. A value of θ which deviates from 0°, 180°, or 90° has for example also been observed by Schreyer *et al.* who reported $\theta=50°$ in the case of Fe/Cr superlattices,[13] but the dependence of the coupling angle on the thickness of the interlayer was so far not reported.

Figure 4 shows the dependence of coupling coefficients C_+ and C_- on the Mn thickness. If the Mn thickness is in the range between 0.62 and 1.2 nm, the oscillations of C_+ and C_- are almost opposite in phase, and vestiges of the short-period coupling can be seen from the shoulders of the curves. If the Mn layer thickness is in the range between 1.2 and 2.45 nm, C_+ and C_- are equal and show short period oscillations of about 2 ML Mn. As was seen in Fig. 3 the remanent state would not reveal these oscillations but they are seen in the saturation field H_S (Fig. 2). Furthermore the Mn thickness dependence of C_- (in Fig. 4) is very similar to that of H_S. For Mn layer thicker than 2.45 nm, no coupling is found at room temperature.

In conclusion, Fe/Mn/Fe wedged-shape sandwiches were prepared by molecular beam epitaxy under optimal conditions. The interlayer coupling measured by magneto-optic Kerr effect is very strong for thin Mn layers. The coupling angle in remanence increases gradually from 0° to about 180° and then gradually reduces to 90° for Mn thicknesses from 0.62 to 1.2 nm. For Mn layer thicknesses in the range between 1.2 and 2.45 nm, the interlayer coupling is always 90° coupling, but its strength oscillates with a short period of about 2 Mn monolayers.

The good agreement between the experimental magnetic hysteresis loops and the theoretical magnetization curves based on the proximity magnetism model implies that the Mn layer in Fe/Mn/Fe trilayers is helicoidal quasiantiferromagnetic[14] at least for thin Mn layers, and the interlayer coupling originates from the direct *d-d* exchange interaction at the Fe-Mn interfaces and propagates through the magnetic ordering of the Mn layer via short-range exchange interaction.

The authors would like to thank D. Olligs, P. Röttländer, U. Rücker, and M. Möller for their help. Shi-shen Yan is pleased to thank the Alexander von Humboldt Foundation for support.

[1] T. G. Walker and H. Hopster, Phys. Rev. B **48**, 3563 (1993).
[2] A. Schreyer *et al.*, Phys. Rev. Lett. **79**, 4914 (1997).
[3] S. T. Purcell *et al.*, Phys. Rev. B **45**, 13 064 (1992).
[4] M. E. Filipkowski, J. J. Krebs, G. A. Prinz, and C. J. Gutierrez, Phys. Rev. Lett. **75**, 1847 (1995).
[5] Q. Wang *et al.*, J. Appl. Phys. **78**, 1689 (1995).
[6] M. Albrecht *et al.*, J. Magn. Magn. Mater. **170**, 67 (1997).
[7] Y. Henry and K. Ounadjela, Phys. Rev. Lett. **76**, 1944 (1996).
[8] J. C. Slonczewski, J. Magn. Magn. Mater. **150**, 13 (1995).
[9] M. Rührig *et al.*, Phys. Status Solidi A **125**, 635 (1991).
[10] J. A. Wolf, Q. Leng, R. Schreiber, P. Grünberg, and W. Zinn, J. Magn. Magn. Mater. **121**, 253 (1993).
[11] M. Schäfer *et al.*, J. Appl. Phys. **77**, 6432 (1995).
[12] R. M. Osgood III, B. M. Clemens, and R. L. White, Phys. Rev. B **55**, 8990 (1997).
[13] A. Schreyer *et al.*, Phys. Rev. B **52**, 16 066 (1995).
[14] D. Stoeffler and F. Gautier, Prog. Theor. Phys. Suppl. **101**, 139 (1990); J. Magn. Magn. Mater. **121**, 259 (1993).